Romanian Reports in Physics **69**, 507 (2017)

NEAR-INFRARED ENERGY BANDGAP BISMUTH OXIDE THIN FILMS AND THEIR IN-DEPTH MORPHO-STRUCTURAL AND OPTICAL ANALYSIS

S. CONDURACHE-BOTA[1], N. TIGAU[1], M. PRAISLER[1], G. PRODAN[2], R. GAVRILA[3]

[1] "Dunarea de Jos" University of Galati, Faculty of Sciences and Environment,
111 Domneasca Street, 800201, Galati, Romania,
E-mails: scondurache@ugal.ro, ntigau@ugal.ro, mirela.praisler@ugal.ro
[2] "Ovidius" University of Constanta, Department of Physics, 124 Mamaia Blvd., 900527 Constanta, Romania, E-mail: gprodan@univ-ovidius.ro
[3] National Institute for Research and Development in Microtechnologies,
126 A Erou Iancu Nicolae Street, 077190, Bucharest, Romania, E-mail: raluca.gavrila@imt.ro

Received September 4, 2016

Abstract. This paper presents the results of the analysis of bismuth oxide thin films prepared by thermal evaporation in vacuum of pure bismuth onto heated glass substrates (from room temperature till 200 °C), followed by thermal oxidation in air. The crystalline structure and the grain size distribution were analyzed by means of transmission electron microscopy and the results were related to the optical properties of the films. The refractive index of the films varies around 2.0 and the energy bandgap (the Wemple-Didomenico model) varies around 1.5 eV, in the near-infrared, making such films useful for thermal energy capture.

Keywords: Bismuth, non-stoichiometric oxides, polymorphism, transmission electron microscopy, Wemple-Didomenico model, energy bandgap.

1. INTRODUCTION

The progress of mankind is measured nowadays also through the progress in Nano- and Optoelectronics. Thin films represent a familiar term in both Science and Technology mainly because they behave differently than their bulk correspondents, due to quantum-size and surface effects, but also since they imply a low quantity of consumed resources, contributing to their savings. Among different materials, oxides proved to be very suitable candidates for thin film deposition and various applications in Optoelectronics, gas sensing, etc. [1–3].

Bismuth oxide is a significant transition metal oxide with large value of energy bandgap, high refractive index, high permittivity, important photosensitivity and photoluminescence and high oxide ionic conductivity at high temperature [4–7], giving its potential and practical use for: optical coatings, solar cells, transparent ceramic glass manufacturing [5], fuel cells and oxygen sensors [8], as

photocatalyst [9] and for data storage [10]. Still, the structure and practically all the physical properties of the films are very sensitive to the deposition method and its particular conditions. Thus, depending on the preparation technique, the electrical conductivity of bismuth oxide may change by five orders of magnitude, while its band gap can vary from 2 to 3.96 eV [11, 12]. Even though there are many applications for bismuth oxide thin films, the problem of the polymorphism of Bi_2O_3 and the possible formation of more than one coexisting intermediate bismuth oxides, such as: BiO, $Bi_2O_{2.33}$, Bi_4O_7, etc makes it very difficult to predict the corresponding physical properties of such complex bismuth oxide thin films.

The properties of materials are directly dependent on their microstructure. X-ray Diffractometry (XRD) gives a lot of structural information on the studied samples, not only on their crystalline phases, crystalline planes, grain sizes, but also on internal tensions and on dislocations density. Still, this information is more an average of the nanoscale features of the analyzed materials. Moreover, XRD cannot assess grain distribution and surely cannot offer a direct inside viewing of the low-scale details of materials. Instead, Transmission Electron Microscopy (TEM) can offer such nanoscale viewing possibilites and through its various techniques has proved an extremely valuable tool for structural analysis at the lowest scale possible. Thus, the very-high magnification TEM images allow for grain distribution assessment, while the SAED technique (Selected Area Electron Diffraction) offers the possibility to examine the structural features much similar to XRD, but on areas as small as a few hundred nm wide.

This paper presents a thorough structural analysis through TEM of bismuth oxide thin films deposited on glass by thermal oxidation of pure bismuth films deposited at different substrate temperatures. The morphology of the films is also studied, since it plays a very important role in the optical properties of thin films. Finally, a fine optical analysis is performed to infer the most relevant optical features of the films, namely their transmittance, refractive index and energy bandgap.

2. EXPERIMENTAL DETAILS

The films under study here were prepared in two stages. The 1st stage consisted in the vacuum thermal evaporation and deposition of pure bismuth thin films onto glass substrates at 0.05 mtorr chamber pressure with an AV 1003 device made by IFA – Atomic Physics Institute from Magurele, Romania. The substrates were kept at different temperatures, T_S during bismuth deposition (300 K – RT = = room temperature, 373 K and 473 K = 200 deg. Celsius). Within the 2nd stage,

the cooled Bi thin films were thermally oxidized in air, by using a home-made annealing device, through one hour gradual heating till 400 ^{o}C and then natural cooling. The oxidation was also visually noticed, wince the films turned from greyish to yellow during the heating process.

The thickness measurements were performed by white-light multiple-beam Fizeau fringes method, by means of a MII-4 Linnik interferential microscope.

The structural analysis of the films was done by using the SAED technique of TEM, at a Philips CM120ST transmission electron microscope. The indexation of the SAED rings was done according to the JCPDS data files from ref. [13], after computing the interplanar distances corresponding to the radius of each electron diffraction ring. The same microscope was used for BF-TEM (bright-field TEM) imaging, at 100 kV electron acceleration voltage.

Atomic Force Microscopy (AFM) was used for the morphological studies, with atomic force microscope with 2 nm vertical resolution and 20 nm lateral resolution, respectively.

Optical transmittance and reflectance measurements with changing wavelength were done with two different spectrophotometers: a Tech5 AG fiber optic spectrophotometer for the transmittance, operating between 300 and 1700 nm, while a STEAG ETA-OPTIK spectrophotometer was employed for reflectance measurements between 400 and 1000 nm. Even though the refractive index, n was inferred by using both the transmittance and reflectance data (see reference [2] for details), the dependence on wavelength of the refractive index is highly similar to the optical reflectance data, on which n depends the most. The model proposed by Wemple-Didomenico was employed for the refractive index of the films, because it allows for a good estimation of their energy bandgap, E_g [14, 15].

3. RESULTS AND DISCUSSION

Figure 1 presents the indexed SAED images of the three types of bismuth oxide films under study, namely those obtained by thermal oxidation in air of pure bismuth films deposited at three substrate temperatures, approximately 100 degrees apart. It can be seen that the one hour heating was not enough for the complete oxidation of any of the bismuth layers. The resulting films present complicated structures, with remanent, un-oxidized Bi mixed with various non-stoichiometric oxides, from the simplest $BiO_{1.5}$ to the complicated $Bi_{12}Bi_{0.8}O_{19.2}$, along with different combinations of bismuth trioxide polymorphs:

- α, β and γ-Bi_2O_3 in the film with $T_S = 300$ K;

- α, β, γ and δ-Bi_2O_3 for the film with $T_S = 373$ K;
- α, β, γ, δ and cubic, c-Bi_2O_3 for the film with $T_S = 373$ K.

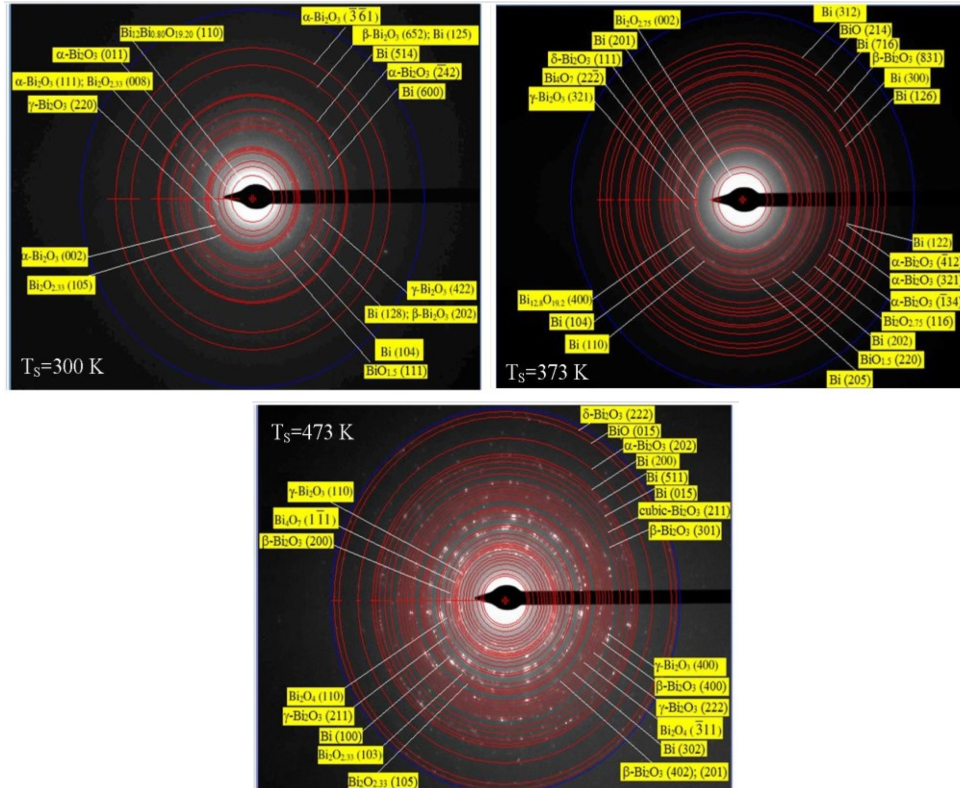

Fig. 1 – SAED images for the bismuth oxide thin films under study.

Moreover, the films are polycrystalline. Thus, for $T_S = 300$ K, one can notice that α-Bi_2O_3 is present in the film with the most numerous crystalline planes: (011), (111), (002), $(\bar{3}\bar{6}1)$ and $(\bar{2}42)$, but β-Bi_2O_3 is also present with (202) and (652) planes, while pure Bi has no less than 4 types of planes in the films. In the case of the film with initial $T_S = 373$ K, pure bismuth has 10 identified crystalline planes, while α-Bi_2O_3 has only three of them: $(\bar{4}12),(321),(\bar{1}34)$, as compared to γ and δ-Bi_2O_3, presenting only one plane each. Finally, the film with initial $T_S = 473$ K, pure Bi exhibits 5 types of crystalline planes, while α-Bi_2O_3 appears only with the (202) plane, γ-Bi_2O_3 shows 3 types of planes, and δ-Bi_2O_3 and cubic-Bi_2O_3 have only one plane each. Such mixed films with bismuth trioxide polymorphs and with the non-stoichiometric bismuth oxides were also reported by

others, prior to thermal stabilization through subsequent annealing of the bismuth oxide films [1, 16]. Thus, there are few, if any structural similarities between the films, proving that the substrate temperature during the initial pure bismuth depositions was crucial for the development of the oxidation process inside the films.

As mentioned above, the grain distribution within the bismuth oxide films could be studied by means of BF-TEM, the corresponding images being shown in Fig. 2, along with the grain histograms, fitted with the Lognormal function.

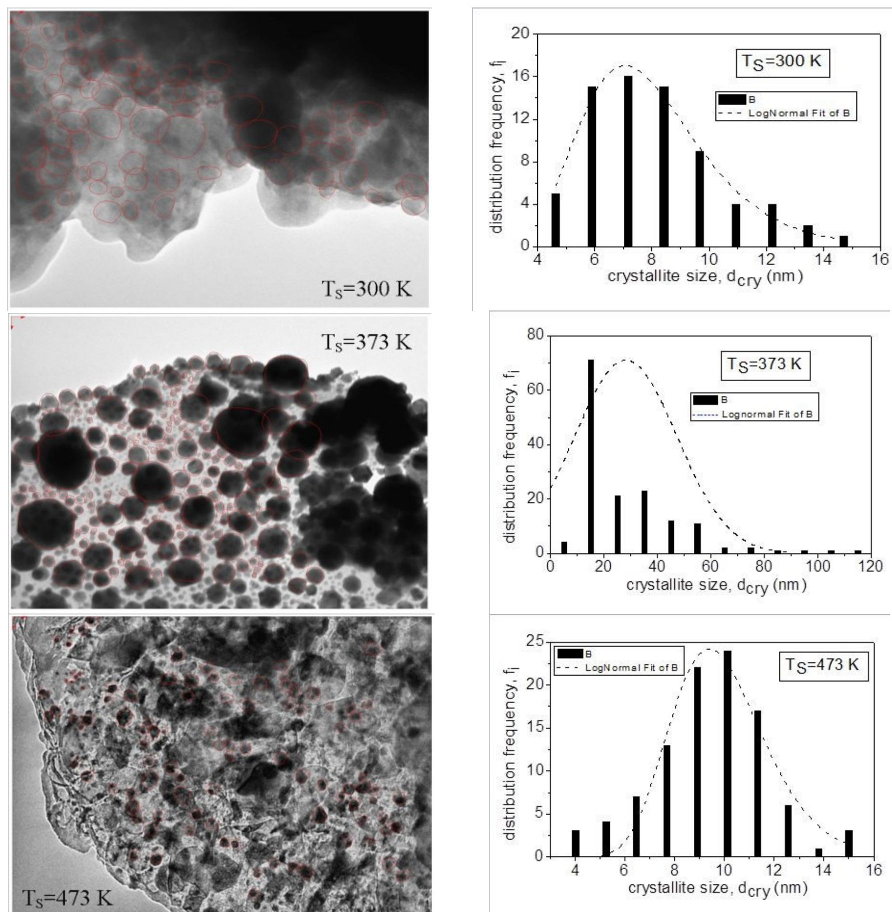

Fig. 2 – BF-TEM images (images from the left) and grain distribution, with Lognormal fit function (images from the right) of the investigated bismuth oxide thin films.

One can see from the graphs at the right side of Fig. 2 that the BF-TEM grain size analysis shows Lognormal-type of size distributions for the films with 300 K

and 473 K initial temperature and a much less normal grain size distribution for the film with $T_S = 373$ K, which can be related to the highest concentration of remanent pure bismuth within this film as compared to the other two.

Table 1 presents some morphological parameters of the bismuth oxide crystalline grains as inferred from the BF-TEM images, namely the mean diameter and the average sphericity of the grains. It can be seen that inside the analyzed depositions, the biggest crystalline grains are obtained for the film prepared through the oxidation of the Bi thin film deposited at 373 K, reaching as much as three times the sizes of the grains from the other two films. The average sphericity of each bismuth oxide films is almost 0.7, given that a perfect spheric grain content would results in an average sphericity of 1.

Table 1

Morphological parameters of the bismuth oxide crystalline grains as inferred from the TEM images

T_S (K)	300	373	473
Mean diameter (nm)	8.20	28.09	9.41
Average sphericity	0.68	0.68	0.65

Figure 3 presents the three-dimensional AFM images of the films under study, at $1\ \mu m \times 1\ \mu m$ scale. Table 2 presents relevant roughness parameters of the films, as inferred from the AFM images, namely: the maximum grain height, the mean roughness of each film's surface, the root mean square roughness (RMS), the asymmetry index (Skewness) and the flatness index (Kurtosis). The Skewness index, R_{sk} is a measure of the profile asymmetry with respect to the center line (*i.e.* the horizontal plane of the sample surface). If $R_{sk} < 0$, this indicates that "valleys" prevail on the surface of the sample. Instead, when $R_{sk} > 0$ this is an indications that "tips" prevails on the surface of the sample. The Kurtosis index, R_{ku} or the flattening index is a measure of the distribution of extremes (tips and valleys) above and below the average line of the profile. Thus, the surfaces with $R_{ku} > 3$ have more peaks/tips, while the surfaces with many valleys have $R_{ku} < 3$.

The AFM surface analysis shows round grains for the films with $T_S = RT$ and 473 K (200 deg. C), as visible in Fig. 4, while the film with T_S = 373 K has a mountain-like surface. Still, from Table 2 it can be seen that the highest grains are not noticed for the film with mountain relief, but instead, for the films with $T_S = 300$ K, the grains surpassing 350 nm height. The same film with $T_S = RT$ has also a more wavy surface, as indicated by its Kurtosis higher than 3 and the highest asymmetry index. The root mean square roughness is also the highest for the film prepared by thermal oxidation of a bismuth layer deposited at room temperature.

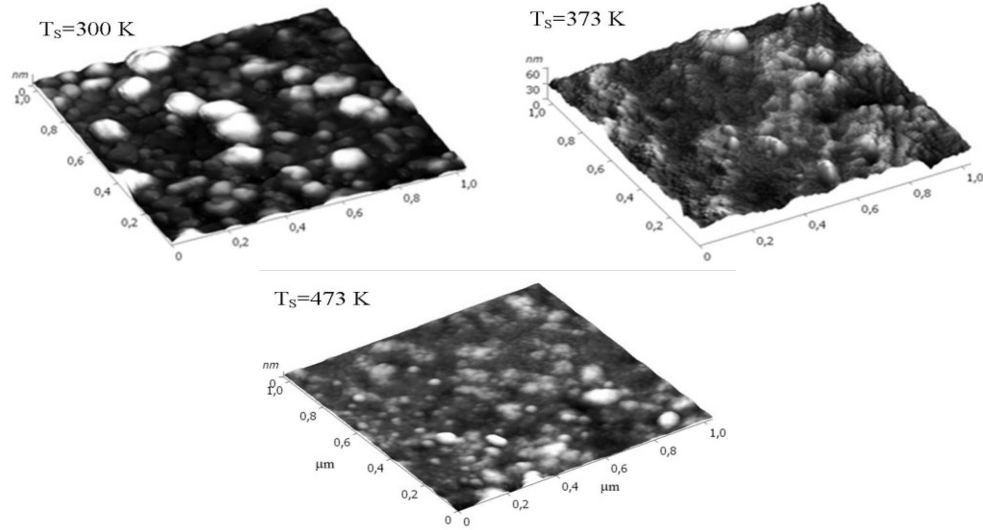

Fig. 3 – Three-dimensional AFM images of the bismuth oxide thin films (1 μm × 1 μm).

By comparing the results of grain distribution as obtained from the BF-TEM data and those concerning the surface roughness distribution, is can be seen that the two distribution are not directly correlated. Thus, while the film with T_s = 373 K has the highest asymmetry in the distribution of its internal grains, instead, the highest surface asymmetry corresponds to the film with $T_s = RT$. Therefore, one cannot conclude about the internal grain distribution from the surface analysis as well as it cannot do the other way around.

Table 2

Roughness parameters of the studied films,
as inferred from the AFM images, at 1 μm × 1 μm scale

T_s (K)	Max. height (nm)	Mean roughness (nm)	RMS (nm)	Skewness, R_{sk}	Kurtosis, R_{ku}
300 (RT)	357.9	17.1	26.3	3.65	25.27
373	62.9	4.5	6.0	0.24	2.21
473	44.5	3.2	4.2	0.75	2.54

Figure 4 presents their optical transmittance spectra in a wide spectral range, proving their relatively good transmittance in the visible and much higher transmittance in the infrared. Each graph from Fig. 4 also contains the thickness of each studied film. It can be seen that the thickness is not the only relevant feature when transmittance is concerned. Thus, the thickest film, with 0.76 micrometers, which corresponds to T_S = 473 K has the highest transmittance above

approximately 600 nm and doesn't go to zero at all in the investigated spectral range. This is not the case with the film having T_S = 373 K which, despite of its small thickness, it has the lowest transmittance, even reaching zero at the end of the Visible.

The refractive index, *n* of the bismuth oxide films presents a peculiar variation with wavelength as passing from one initial substrate temperature to another (Fig. 5). Thus, while the refractive index is roughly constant for the films with T_S = *RT* and 473 K, films that have round grains at the surface, instead, the film with T_S = 373 K, having a mountain-like surface, shows oscillations for its refractive index, with anomalous dispersion on some narrow spectral regions. The values of n increase from the film with T_S = *RT* to the film with T_S = 473 K, while the film with T_S = 373 K has on narrow spectral ranges, higher or smaller values of n as compared to the other two films.

Following the application of the Wemple-Didomenico model, the optical energy band gap of the studied films was inferred, as presented in Table 3.

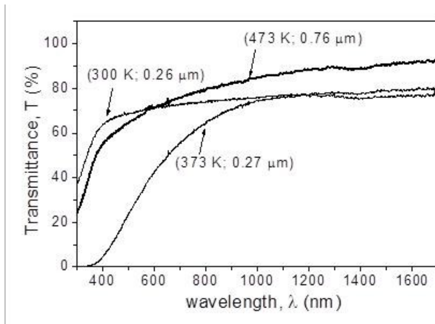

Fig. 4 – The optical transmittance spectra of the bismuth oxide thin films.

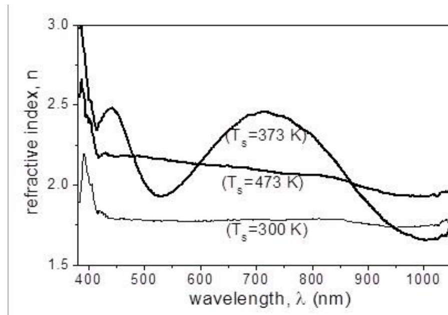

Fig. 5 – Refractive index of the investigated films in the NIR-VIS-NUV range.

Table 3

Optical energy bandgap of the studied films

T_S (K)	Energy bandgap, E_g (eV)
300 (RT)	1.63
373	1.53
473	1.67

From Table 3 it can be concluded that all the analyzed films exhibit a semiconductor behavior, with energy bandgaps around 1.5 eV, suitable for near-infrared applications, such as thermal energy capture. The film with mountain-like structure has the smallest E_g from all the analyzed films (1.53 eV), but the changes in E_g from one film to another are rather insignificant. Such a small energy

bandgap is due to the high content of remanent un-oxidized bismuth within the films treated in air. It is to be expected that these films would be dominated by indirect allowed transitions. This is because the films possess complicated composition and structure, which determines a complex structure for the energy bands, with intermediate energy levels in the forbidden bandgap, as given by the different oxides formed within the films.

4. CONCLUSIONS

This paper proves that there is a strong dependence especially of the morpho-structural, but also of the optical properties of bismuth oxide thin films on the temperature of the glass substrate during the initial bismuth deposition. The SAED technique associated to a Transmission Electron Microscope proves to be a valuable tool for thin film structural analysis, in more detail than with X-ray Diffraction. The analysis pointed out that the films are incompletely oxidized, with non-stoichiometric oxides within, associated polymorphism and polycrystallinity. This is a typical behavior for bismuth while oxidized, as reported by others [17–20]. The BF-TEM grain size analysis shows Lognormal-type of size distributions for the films with T_S = 300 K and 473 K during initial bismuth deposition on glass. Inside the depositions, the biggest crystalline grains are obtained for the film prepared from the Bi thin film deposited at 373 K.

The AFM surface analysis shows different morphologies of the films, depending on their initial substrate temperature. Thus, round grains are found at the surface of the films with $T_S = RT$ and 473 K, while compact, mountain-like surface is noticed for the film with T_S = 373 K. Still, the highest grains are observed for the film with T_S = 300 K, along with a wavy surface.

The optical transmittance of the films depends more on the preparation conditions than on the thickness of the films. The highest transmittance is obtained for the film with T_S = 473 K, even though it is the thickest of all. Depending on the morphology of the films, the refractive index changes differently with wavelengths for the three types of studied films. Thus, the films with round grains on the surface have almost constant refractive index over a wide spectral range, while the film with mountain-like surface exhibits an oscillating refractive index and anomalous dispersion along some narrow spectral regions. The energy bandgap of the films is around 1.5 eV, the lowest value being reached for the film with mountain-like morphology. No reports on such low energy bandgaps were found in the literature for bismuth oxide thin films.

Most surely, the films need structural stabilization through annealing, after which such semiconducting films will be useful for various optoelectronic applications, depending on the preparation conditions, which can be chosen such as the resulting properties to be tuned as required for Science and/or Technology.

Acknowledgments. The work of Simona Bota (Condurache-Bota) has been funded by the Sectoral Operational Programme Human Resources Development 2007-2013 of the Ministry of European funds through the Financial Agreement POSDRU/159/1.5/S/132397.

REFERENCES

1. R. B. Patil, R. K. Puri, V. Puri, Appl. Surf. Sci. **253**, 8682–8688 (2007).
2. S. Condurache-Bota, N. Tigau, A. P. Rambu, G. G. Rusu, G. I. Rusu, Appl. Surf. Sci. **257**, 10545–10550 (2011).
3. M. Karthika, V. Manoj, S. Boomadevi, K. Jeyadheepan, R.K. Karn, R. John Bosco Balaguru, S.K. Pandiyan, Asian J. Appl. Sci. **7**(8), 786–791 (2014).
4. J. Morasch, S. Li, J. Brotz, W. Jaegermann, A. Klein, Phys. Status Solidi A **211**(10), 93–100 (2014).
5. L. Leontie, M. Caraman, A. Vişinoiu, G. I. Rusu, Thin Solid Films **473**, 230–235 (2005).
6. H.T. Fan, X.M. Teng, S.S. Pan, C. Ye, G.H. Li, L.D. Zhang, Appl. Phys. Lett. **87**, 231916–231918 (2005).
7. S.S. Bhande, R.S. Mane, A.V. Ghule and S.-H. Han, Scripta Mater. **65**, 1081–1084 (2011).
8. T. P. Gujar, V. R. Shinde, C. D. Lokhande, Mater. Res. Bull. **41**(8), 1558–1564 (2006).
9. C.-H. Ho, C.-H. Chan, Y.-S. Huang, L.-C. Tien, L.-C. Chao, Opt. Express **21**(10), 11965–11972 (2013).
10. Jiang, Z., Geng, Y., Gu, D., Chinese Opt. Lett. **6,** 294–296 (2008).
11. T. P. Gujar, V. R. Shinde, C.D. Lokhande, Appl. Surf. Sci. **254**, 4186–490 (2008).
12. P. Shuk, H.-D. Wiemhofer, U. Guth, W. Göpel, M. Greenblatt, Solid State Ionics **89**, 179 (1996).
13. JCPDS data files nos. 01-0688, 05-0519, 18-244, 27-49, 27-50, 27-51, 27-52, 27-54, 29-236, 41-1449, 44-1246, 45-1344, 47-1057, 47-1058, 71-0465, 71-0466, 71-0467, 71-2274, 72-0398, 74-1373, 74-1375, 74-1633, 74-1999, 74-2352, 75-0993, 75-0995, 76-1730, 77-0374, 77-0868, 77-2008, 78-0736, 81-0563, 83-0410, 85-1329.
14. F. Yakuphanoglu, M. Durmus, M. Okutan, O. Koysal and V. Ahsen, Physica B: Condens. Matter. **373**(2), 262–266 (2006).
15. S. Condurache-Bota, G. I. Rusu, N. Tigau and L. Leontie, Cryst. Res. Technol. **45**(5), 503–511 (2010).
16. E.T. Al Waisy and M.S. Al Wazny, J. Univ. Anbar Pure Sci. **7**(2), 1–3 (2013).
17. C. L. Gomez, Osmary Depablos-Rivera, P. Silva-Bermudez, S. Muhl, A. Zeinert, M. Lejeune, S. Charvet, P. Barroy, E. Camps, S. E. Rodil, Thin Solid Films **578**, 103–112 (2015).
18. F. Schroder, N. Bagdassarov, F. Ritter, L. Bayarjargal, Phase Tranzit. **83**(5), 311–325 (2010).
19. C.M.B. Hincapié, M.J.P. Cárdenas, J.E.A. Orjuela, E.R. Parra and J.J.O. Florez, Dyna **176**, 139–148 (2012).
20. A. J. Salazar-Perez, M. A. Camacho-Lopez, R. A. Morales-Luckie, V. Sanchez-Mendieta, F. Urena Nunez, J. Arenas Alatorre, Superficies y Vacio **18**(3), 4–8 (2005).